increases. Indeed, the complexes of the metals from the lowest group number considered, Tc^{II} and Re^{II}, have C–S bonds that are amongst the longest, despite having one less electron in the t_{2g} orbitals than all other complexes in the series. As this trend continues, at some point C–S bond lengthening might be sufficient to cause complete cleavage of the bond. This is indeed observed: reduction of yellow $[Re(9S3)_2]^{2+}$ [7] in water with ascorbic acid, at room temperature, immediately induces cleavage of two C–S bonds of one 9S3 ligand to give ethene and the yellow-brown rhenium(III) dithiolate complex $[Re(9S3)(SCH_2CH_2SCH_2CH_2S)]^+$ in 90% yield of the isolated BF_4 salt [Eq. (a)]. The structure of the product has been determined by X-ray crystallography[8] and is shown in Figure 5 together with pertinent bond lengths and angles. The structural dimensions indicate nearly ideal octahedral coordination, with very little change relative to $[Re(9S3)_2]^{2+}$ except for the loss of ethene.

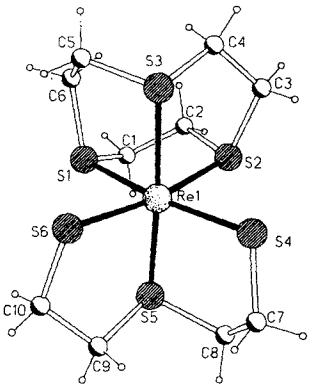

Figure 5. Structure of $[Re(9S3)(SCH_2CH_2SCH_2CH_2S)]^+$. Pertinent bond lengths (Å): Re–S1 2.436(2); Re–S2 2.463(2); Re–S3 2.393(2); Re–S4 2.256(2); Re–S5 2.346(2); Re–S6 2.272(2); S1–C1 1.822(8); S1–C6 1.829(9); S2–C2 1.819(9); S2–C3 1.818(9); S3–C4 1.847(9); S3–C5 1.830(8).

$$[Re(9S3)_2]^{2+} + e \longrightarrow "[Re(9S3)_2]^{+}" \longrightarrow [Re(9S3)(SCH_2CH_2SCH_2CH_2S)]^+ + C_2H_4 \quad (a)$$

The ethene was collected quantitatively and identified by gas chromatography/mass spectrometry. We have also shown that the analogous yellow technetium complex $[Tc(9S3)_2]^{2+}$ [9] behaves similarly, giving the pink complex $[Tc(9S3)(SCH_2CH_2SCH_2CH_2S)]^+$. That the C–S cleavage is simply the consequence of electron transfer to $[M(9S3)_2]^{2+}$, and not a more complex reaction involving ascorbic acid specifically, was demonstrated when the same products were isolated from the reaction of the rhenium complex with various other reducing agents including metallic zinc and chromium (in the case of rhenium) or stannous chloride (in the case of technetium). Similarly, if $[Re(9S3)_2]^{2+}$ is reduced electrochemically at a platinum electrode, bubbles of ethene can be seen to evolve at the electrode surface. A search for ethene production by similar ascorbate treatment of 9S3 complexes containing metals further to the right in the d-block (Rh^{III}, Fe^{II}) failed to find ethene. It thus appears that addition of the sixth electron to the t_{2g} orbitals causes the back-donation to become so strong that occupancy of the C–S σ^* orbital is enough to cancel the C–S bond and release ethene, provided the t_{2g} orbitals have high enough energy. Fast-atom-bombardment (FAB) mass spectroscopy indicates that further loss of ethene molecules from $[Re(9S3)(SCH_2CH_2SCH_2CH_2S)]^+$ occurs in the spectrometer: peaks appear at 519 (M^+, 100%), 491 ($M^+ - C_2H_4$), 463 ($M^+ - 2(C_2H_4)$), 435 ($M^+ - 3(C_2H_4)$), 403 ($M^+ - 3(C_2H_4) - S$), and 375 ($M^+ - 4(C_2H_4) - S$). The precursor complex $[Re(9S3)_2]^{2+}$ also undergoes serial losses of ethene in the FAB mass spectrometer.

The combined structural and chemical patterns described here provide compelling experimental evidence to support the computational arguments not only that the thioether ligand acts as a π-acceptor ligand in thioether complexes (especially where the d orbitals of the metal have relatively high energy) but also that the ligand π-acceptor orbitals have considerable C–S σ^* character and can accept sufficient electron density to achieve complete C–S bond cleavage.

Experimental Section

Structural parameters were obtained from the Cambridge Crystallographic Data Centre. To identify in-plane and out-of-plane C–S bonds, the pictures of the structures were assembled and studied on computer (Iris Indigo^2 workstation, Silicon Graphics).

Synthesis: To a solution of $[Re(9S3)_2][BF_4]_2$ (200 mg, 0.27 mmol) in water (5 mL) was added L-ascorbic acid (80 mg, 0.45 mmol). After stirring for 2 h the red-brown solid was collected and dried in vacuo. Recrystallization from water gave $[Re(9S3)(SCH_2CH_2SCH_2CH_2S)][BF_4]$ (140 mg, 86%) in the form of crystals suitable for X-ray analysis. Elemental analysis calcd: C 31.7, H 5.3; found: C 31.6, H 5.2.

Received: November 25, 1996 [Z98191E]
German version: *Angew. Chem.* **1997**, *109*, 1254–1256

Keywords: bond theory · rhenium · technetium · S ligands

[1] A. G. Orpen, N. G. Connelly, *J. Chem. Soc. Chem. Commun.* **1985**, 1310–1311.
[2] D. S. Marynick, *J. Am. Chem. Soc.* **1984**, *106*, 4064–4065.
[3] S.-X. Xiao, W. C. Trogler, D. E. Ellis, Z. Berkovitch-Yellin, *J. Am. Chem. Soc.* **1983**, *105*, 7033–7037.
[4] H.-B. Kraatz, H. Jacobsen, T. Ziegler, P. H. Boorman, *Organometallics* **1993**, *12*, 76–80.
[5] S. R. Cooper, S. C. Rawle, *Struct. Bonding (Berlin)* **1990**, *72*, 1–72.
[6] Quanta, version 4.1, Biosym/Molecular Simulations, San Diego, CA, USA, **1995**.
[7] S. R. Cooper, S. O. C. Matondo, P. Mountford, D. J. Watkin, W. B. Jones, *J. Chem. Soc. Chem Commun.* **1995**, 161–162.
[8] Crystal structure data: $C_{10}H_{20}BF_4ReS_6$; crystal dimensions $0.3 \times 0.2 \times 0.1$ mm; orthorhombic, *Pbca* (no. 61); $a = 12.091(2)$, $b = 14.223(3)$, $c = 20.534(4)$ Å; $V = 3.531.2(12)$ Å^3, $Z = 8$; $\rho_{calcd} = 2.278$ gcm^{-3}; $5.2° < 2\theta < 50°$; $Mo_{K\alpha}$ irradiation, $\lambda = 0.71073$ Å; ω scans; $T = 293$ K; 3107 reflections (2157 with $F > 4\sigma(F)$; Lorentzian polarization and absorption corrections (ψ scans) were applied; $\mu = 7.619$ mm^{-1}, min/max transmission factors 0.785–1.000. Structure solution was by direct methods (SIR92), least squares refinement on F^2 (SHELXTLplus) on 197 parameters on $F > 4\sigma(F)$ gave $R1 = 0.0360$, wR on F^2 for all data = 0.1047. Hydrogen atoms were included at calculated positions. Largest peak/hole in residual electron density map ± 1.890 e Å^{-3}. Crystallographic data (excluding structure factors) for the structure reported in this paper have been deposited with the Cambridge Crystallographic Data Centre as supplementary publication no. CCDC-100221. Copies of the data can be obtained free of charge on application to The Director, CCDC, 12 Union Road, Cambridge CB2 1EZ (fax: int. code +(1223)336-033; e-mail: deposit@chemcrys.cam.ac.uk).
[9] D. J. White, H.-J. Küppers, A. J. Edwards, D. J. Watkin, S. R. Cooper, *Inorg. Chem.* **1992**, *31*, 5351–5352.

Highly Enantioselective Reduction with Novel, Bridged NADH Models**

Nobuhiro Kanomata* and Tadashi Nakata

An L-lactate dehydrogenase that requires the coenzyme NADH catalyzes enantioselective reduction of pyruvate to L-lactate in anaerobic glycolysis. The enzymatic environment in this reaction fulfills the most important factors for asymmetric

[*] Dr. N. Kanomata, Prof. Dr. T. Nakata
The Institute of Physical and Chemical Research (RIKEN)
Wako-shi, Saitama 351-01 (Japan)
Fax: Int. code +(48)462-4666
e-mail: nobkano@riken.go.jp

[**] N. K. gratefully acknowledges financial support by a Grant-in-aid for Science Research from Ministry of Education, Science, and Culture (no. 07740514) and a Special Grant for Promotion of Research from The Institute of Physical and Chemical Research (RIKEN). N. K. is a Special Researcher in the Basic Science Program, RIKEN (1994–1997). We thank Ms. Kimiko Kobayashi, RIKEN, for the X-ray crystallographic analysis.

  0570-0833/97/3611-1207 $ 17.50+.50/0

induction: stereoselective transfer of one of the diastereotopic hydrogen atoms in NADH to achiral substrates and controlled orientation of substrate approach (*re*- or *si*-face selectivity for the substrates). Many organic and bioorganic chemists have been challenged to mimic this biochemical reaction with various NADH models[1–7] that aid in reducing pyruvate analogs with high enantioselectivity. Interpretation of the enzymatic function in asymmetric reduction with coenzyme NADH led us to design novel, bridged NADH models[8] with an [*n*](2,5)pyridinophane (parapyridinophane) skeleton[9] as promising candidates for recyclable compounds that induce high enantioselectivity. The oligomethylene chain bridging the 2- and 5-positions of a dihydronicotinoyl ring would behave as an "enzyme wall" that allows the substrates to approach from the opposite side exclusively (Scheme 1). We describe here the syntheses of homochiral, bridged NADH models and their outstanding ability to reduce methyl benzoylformate, an analog of pyruvic acid, with high enantioselectivity.

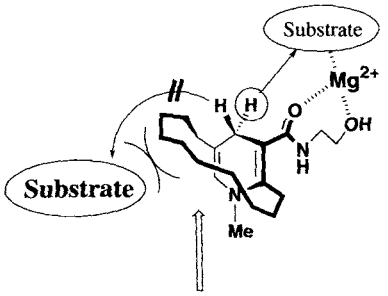

Scheme 1. Protection of one side of the dihydronicotinoyl ring in bridged NADH model compounds by the oligomethylene bridge.

The synthesis of the bridged nicotinate **12**, a key synthetic intermediate toward NADH models **16**, is outlined in Scheme 2. *cis*-2-Chlorocyclododecene-1-carboxaldehyde (**1**)[10] was treated with sodium azide and a catalytic amount of lithium chloride to give azirine **2**[11] and *trans*-2-azidocyclododecene-1-carboxaldehyde (**3**)[12] in a 61:39 ratio.[13] Subsequent irradiation of the mixture in chloroform resulted in conversion of **3** into **2** (84% yield based on **1**). The thermal ring-opening reaction of **2** with triphenylphosphane proceeded in toluene at reflux to give the iminophosphorane **4**[14] in 84% yield. The ^{1}H NMR spectrum of **4** shows that it is a mixture of *cis* and *trans* isomers in a ratio of about 1:3, based on their aldehyde signals at $\delta = 10.66$ (0.25H) and 9.87 (0.75H), respectively.[15]

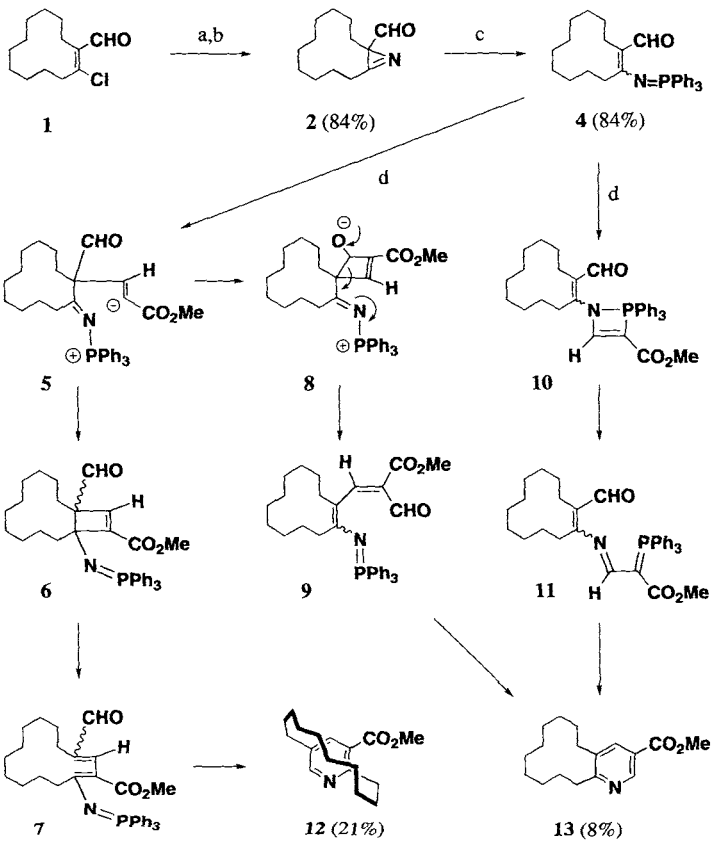

Scheme 2. Synthesis of nicotinates **12** and **13**. a) NaN_3, LiCl (cat.), H_2O, THF, RT, 5 h; b) *hν* (Pyrex), $CHCl_3$, RT, 8 h; c) PPh_3, toluene, Δ, 3 h; d) methyl propiolate (10 equiv), toluene, 140 °C, 12 h.

Methyl [10](2,5)pyridinophane-3-carboxylate (**12**) was synthesized from **4** and methyl propiolate (10 equivalents) in toluene at 140 °C. The desired product was obtained in 21% yield along with its *ortho*-bridged isomer **13** (8%). The structures of these compounds were deduced by ^{1}H and ^{13}C NMR and mass spectroscopy (see Table 1). The ^{1}H NMR spectrum of **12** shows that one of oligomethylene protons ($\delta = 0.13$) is located in a shielded area above the pyridine ring. Furthermore, all the bridge protons appear as independent signals, in accordance with a nonsymmetric structure. This indicates that **12** has a parapyridinophane skeleton with no flipping (*jump-rope rotation*) of the oligomethylene bridge on the NMR time scale. All other spectroscopic data agree with the proposed structure of **12**. As for **13**, geminal methylene protons of the oligomethylene bridge afford identical chemical shifts due to the symmetrical structure, which is in contrast to **12**.

The postulated pathways for this novel pyridine-formation reaction are also depicted in Scheme 2. Enamine-type addition of **4** to the β position of methyl propiolate provided intermediate **5**; intramolecular addition on the C=N and C=O bonds produced cyclobutene intermediates **6** and **8**, respectively. Spontaneous ring opening of **6** and **8** generated (vinylimino)phosphoranes **7** and **9**, which underwent intramolecular aza-Wittig reactions to give pyridines **12** and **13**. Formation of a portion of **13** can also be explained by initial cycloaddition of methyl propiolate to the N=P bond of **4** to give **10**. Subsequent cycloreversion of **10** and intramolecular Wittig reaction of **11** afforded **13**. Similar pyridine formation occurred in the reaction of **4** with dimethyl acetylenedicarboxylate (2 equivalents) to give both isomers of *ortho*-bridged 3,4- and 2,3-pyridinedicarboxylates (5% and 14%, respectively) in addition to [10](2,5)pyridinophane-3,4-dicarboxylate (14%). Formation of the two *ortho*-bridged nicotinates suggests that there are also two independent routes from **4** to **13**.

Conversion of **12** into the NADH models **16** was accomplished by transformation of the ester to an amide followed by *N*-alkylation and selective reduction of the pyridinium rings (Scheme 3). Hydrolysis of **12** with lithium hydroxide afforded the corresponding nicotinic acid (81%), and the amide formation reaction with (*S*)-valinol gave diastereomeric nicotinamides **14**, which were separated to give (*S,S*)-**14** and (*R,S*)-**14** in 48% yield each. Once purified these compounds are stable enough at room temperature that no flipping of the oligomethylene bridge occurs. This is in contrast to 2,8-dithia[10](2,5)pyridinophane,[9d] which undergoes racemization. Thermal interconversion between (*S,S*)- and (*R,S*)-**14** is observed in toluene at reflux and reaches equilibrium after 8 h to give a nearly 1:1 mixture. This phenomenon is remarkably useful for the selective preparation of homochiral **14**, since repeated "separation and interconversion" could result in either (*S,S*)- or (*R,S*)-**14**.

The structure of (*S,S*)-**14** was unequivocally solved by X-ray crystallographic analysis of colorless plates obtained by recrystallization from ethyl acetate (Figure 1).[16] The interesting feature of the structure is that the thermal vibration of the

  0570-0833/97/3611-1208 $ 17.50+.50/0

Table 1. Selected spectroscopic data for **12**–**16**.

12: Oil; ^{1}H NMR (500 MHz, $CDCl_3$): $\delta = 0.13$ (m, 1H), 0.50 (m, 1H), 0.64 (m, 1H), 0.70–0.77 (m, 3H), 0.83 (m, 2H), 1.07–1.16 (m, 3H), 1.23 (m, 1H), 1.46 (m, 2H), 1.80 (m, 1H), 1.86 (m, 1H), 2.63 (ddd, $J = 13.5$, 10.3, 4.3 Hz, 1H), 2.75 (ddd, $J = 13.5$, 6.0, 4.3 Hz, 1H), 2.79 (ddd, $J = 12.8$, 10.3, 4.3 Hz, 1H), 3.80 (ddd, $J = 12.8$, 6.4, 4.3 Hz, 1H), 3.93 (s, 3H), 8.01 (d, $J = 2.1$ Hz, 1H), 8.46 (d, $J = 2.1$ Hz, 1H); ^{13}C NMR (125 MHz, $CDCl_3$): $\delta = 24.5$, 25.3, 26.3, 26.5, 27.71, 27.73, 28.0, 28.2, 31.9, 36.1, 52.2, 125.3, 134.4, 138.8, 151.9, 161.5, 167.2; MS (EI): m/z (%): 275 (94) [M^+], 216 (100)

13: Yellow solid; ^{1}H NMR (500 MHz, $CDCl_3$): $\delta = 1.41$ (m, 8H), 1.51 (m, 4H), 1.75 (m, 2H), 1.88 (m, 2H), 2.72 (t, $J = 7.7$ Hz, 2H), 2.89 (t, $J = 7.7$ Hz, 2H), 3.93 (s, 3H), 8.07 (d, $J = 2.2$ Hz, 1H), 8.98 (d, $J = 2.2$ Hz, 1H); ^{13}C NMR (125 MHz, $CDCl_3$): $\delta = 22.85$, 22.93, 24.9, 25.3, 25.7, 26.0, 27.8, 28.8, 29.1, 31.8, 52.1, 123.4, 135.9, 138.1, 147.8, 165.4, 166.2; MS (EI): m/z (%): 275 (59) [M^+], 165 (100)

(*S,S*)-**14**: Colorless plates; ^{1}H NMR (500 MHz, $CDCl_3$): $\delta = 0.36$ (m, 1H), 0.52–0.63 (m, 2H), 0.72–0.85 (m, 5H), 1.04 (d, $J = 6.8$ Hz, 3H), 1.05 (d, $J = 6.8$ Hz, 3H), 1.12 (m, 2H), 1.21 (m, 2H), 1.45 (m, 1H), 1.65 (m, 1H), 1.80 (m, 2H), 2.02 (oct., $J = 6.8$ Hz, 1H), 2.61 (ddd, $J = 13.7$, 10.0, 4.3 Hz, 1H), 2.73 (ddd, $J = 13.7$, 6.3, 4.4 Hz, 1H), 2.85 (ddd, $J = 13.0$, 9.0, 4.3 Hz, 1H), 3.26 (ddd, $J = 13.0$, 8.0, 4.4 Hz, 1H), 3.78 (dd, $J = 11.1$, 5.8 Hz, 1H), 3.82 (dd, $J = 11.1$, 3.4 Hz, 1H), 3.96 (dddd, $J = 8.1$, 6.8, 5.8, 3.4 Hz, 1H), 6.01 (br d, $J = 8.1$ Hz, 1H), 7.56 (d, $J = 2.1$ Hz, 1H), 8.41 (d, $J = 2.1$ Hz, 1H); ^{13}C NMR (125 MHz, $CDCl_3$): $\delta = 19.0$, 19.7, 24.7, 25.2, 26.4, 26.5, 27.7, 27.8, 27.9, 28.3, 29.2, 31.9, 35.1, 57.6, 63.8, 132.2, 134.7, 135.8, 150.4, 157.7, 169.5; $[\alpha]_D^{26} = +64.9$ ($c = 1$ in $CHCl_3$); MS (EI): m/z (%): 346 (31) [M^+], 244 (100)

(*R,S*)-**14**: Oil; ^{1}H NMR (500 MHz, $CDCl_3$): $\delta = 0.35$ (m, 1H), 0.53 (m, 1H), 0.60 (m, 1H), 0.71–0.85 (m, 5H), 1.01 (d, $J = 6.8$ Hz, 3H), 1.04 (d, $J = 6.8$ Hz, 3H), 1.06–1.26 (m, 4H), 1.44 (m, 1H), 1.64 (m, 1H), 1.79 (m, 2H), 2.00 (oct., $J = 6.8$ Hz, 1H), 2.60 (ddd, $J = 13.3$, 10.3, 6.3 Hz, 1H), 2.71 (ddd, $J = 13.3$, 5.6, 5.1 Hz, 1H), 2.83 (ddd, $J = 13.3$, 9.0, 3.9 Hz, 1H), 3.27 (ddd, $J = 13.3$, 7.5, 4.1 Hz, 1H), 3.80 (dd, $J = 11.3$, 5.6 Hz, 1H), 3.85 (dd, $J = 11.3$, 3.4 Hz, 1H), 3.97 (dddd, $J = 8.6$, 6.8, 5.6, 3.4 Hz, 1H), 6.12 (br. d, $J = 8.6$ Hz, 1H), 7.53 (d, $J = 2.1$ Hz, 1H), 8.39 (d, $J = 2.1$ Hz, 1H); ^{13}C NMR (125 MHz, $CDCl_3$): $\delta = 18.9$, 19.6, 24.6, 25.2, 26.4, 26.5, 27.7, 27.8, 27.9, 28.3, 29.1, 31.9, 34.9, 57.4, 63.6, 132.2, 134.7, 135.8, 150.2, 157.3, 169.3; $[\alpha]_D^{26} = -80.1$ ($c = 1$ in $CHCl_3$); MS (EI): m/z (%): 346 (35) [M^+], 244 (100)

(*S,S*)-**15a**: Yellow solid; ^{1}H NMR (500 MHz, $CDCl_3$): $\delta = -0.03$ (m, 1H), 0.68–0.95 (m, 7H), 1.05 (d, $J = 6.8$ Hz, 3H), 1.07 (d, $J = 6.8$ Hz, 3H), 1.09–1.28 (m, 4H), 1.55 (m, 1H), 1.73 (m, 1H), 1.79 (m, 1H), 2.01, (m, 1H), 2.10 (oct., $J = 6.8$ Hz, 1H), 2.82 (ddd, $J = 14.0$, 9.2, 4.9 Hz, 1H), 2.96 (ddd, $J = 14.0$, 7.0, 5.2 Hz, 1H), 3.43 (ddd, $J = 15.3$, 5.2, 4.9 Hz, 1H), 3.58 (ddd, $J = 15.3$, 10.4, 5.2 Hz, 1H), 3.77 (dd, $J = 11.9$, 3.7 Hz, 1H), 3.81 (dd, $J = 11.9$, 6.4 Hz, 1H), 3.93 (dddd, $J = 7.9$, 6.8, 6.4, 3.7 Hz, 1H), 4.42 (s, 3H), 8.31 (s, 1H), 8.34 (d, $J = 7.9$ Hz, 1H), 8.46 (s, 1H); ^{13}C NMR (68 MHz, $CDCl_3$): $\delta = 19.7$, 19.8, 24.1, 25.0, 25.9 (2C), 26.0, 26.87, 26.90, 27.8, 29.3, 31.2, 32.0, 47.1, 58.9, 62.7, 139.5, 140.8, 145.2, 145.5, 155.6, 164.8; $[\alpha]_D^{23} = +61.8$ ($c = 1$ in $CHCl_3$); MS (ESI): m/z (%): 361 (100) [$M - I^-$]; MS (ESI, negative ion): m/z (%): 615 (100) [$M + I^-$], 127 (35) [I^-]

(*S,S*)-**15b**: MS (ESI, negative ion): m/z (%): 559 (62) [$M + ClO_4^-$], 99 (100) [ClO_4^-]

(*R,S*)-**15a**: Yellow solid; ^{1}H NMR (500 MHz, $CDCl_3$): $\delta = -0.12$ (m, 1H), 0.70–0.99 (m, 7H), 1.01 (d, $J = 6.8$ Hz, 3H), 1.02 (d, $J = 6.8$ Hz, 3H), 1.12–1.28 (m, 4H), 1.55 (m, 1H), 1.73 (m, 1H), 1.79 (m, 1H), 1.98, (oct., $J = 6.8$ Hz, 1H), 2.04 (m, 1H), 2.83 (ddd, $J = 14.3$, 8.8, 5.2 Hz, 1H), 2.94 (ddd, $J = 14.3$, 7.3, 5.4 Hz, 1H), 3.00 (dd, $J = 7.6$, 6.7 Hz, 1H), 3.46 (dt, $J = 15.3$, 5.2 Hz, 1H), 3.58 (ddd, $J = 15.3$, 10.3, 5.4 Hz, 1H), 3.80 (ddd, $J = 11.9$, 6.7, 3.7 Hz, 1H), 3.86 (dt, $J = 11.9$, 7.6 Hz, 1H), 4.01 (ddd, $J = 7.6$, 6.8, 3.7 Hz, 1H), 4.42 (s, 3H), 8.07–8.11 (br. s, 1H), 8.09 (d, $J = 1.5$ Hz, 1H), 8.40 (d, $J = 1.5$ Hz, 1H); ^{13}C NMR (68 MHz, $CDCl_3$): $\delta = 19.4$, 19.5, 24.1, 24.9, 25.88, 25.93, 26.1, 26.8, 26.9, 28.0, 29.4, 31.3, 32.5, 47.2, 58.6, 62.3, 139.9, 140.7, 143.5, 145.0, 156.6, 164.8; $[\alpha]_D^{26} = -75.4$ ($c = 1$ in $CHCl_3$); MS (ESI): m/z (%): 361 (100) [$M - I^-$]; MS (ESI, negative ion): m/z (%): 615 (100) [$M + I^-$], 127 (35) [I^-]

(*R,S*)-**15b**: MS (ESI, negative ion): m/z (%) 559 (38) [$M + ClO_4^-$], 99 (100) [ClO_4^-]

(*S,S*)-**16**: Oil; ^{1}H NMR (500 MHz, $CDCl_3$): $\delta = 0.85$–1.65 (m, 16H), 0.95 (d, $J = 6.8$ Hz, 3H), 3H, 0.98 (d, $J = 6.8$ Hz, 3H), 1.95 (oct., $J = 6.8$ Hz, 1H), 2.05 (ddd, $J = 13.7$, 12.4, 4.7 Hz, 1H), 2.15 (dtd, $J = 13.7$, 3.2, 1.7 Hz, 1H), 2.25 (dtd, $J = 14.5$, 4.3, 1.8 Hz, 1H), 2.79 (br. d, $J = 16.3$ Hz, 1H), 2.90 (dd, $J = 16.3$, 0.9 Hz, 1H), 3.07 (s, 3H), 3.45 (ddd, $J = 14.5$, 11.5, 4.1 Hz, 1H), 3.52 (m, 1H), 3.59 (m, 1H), 3.66–3.72 (m, 2H), 5.60 (br. d, $J = 6.0$ Hz, 1H), 5.73 (d, $J = 0.9$ Hz, 1H); ^{13}C NMR (125 MHz, $CDCl_3$): $\delta = 18.5$, 19.7, 23.6, 25.1, 25.5, 25.7, 26.7, 27.03, 27.04, 27.2, 27.82, 27.83, 29.3, 30.7, 36.7, 58.1, 65.6, 101.3, 109.6, 130.6, 147.7, 172.8

(*R,S*)-**16**: Oil; ^{1}H NMR (500 MHz, $CDCl_3$): $\delta = 0.84$–1.65 (m, 16H), 0.95 (d, $J = 6.8$ Hz, 3H), 0.97 (d, $J = 6.8$ Hz, 3H), 1.89 (oct., $J = 6.8$ Hz, 1H), 2.05 (ddd, $J = 13.2$, 12.4, 4.7 Hz, 1H), 2.15 (br. d, $J = 12.4$ Hz, 1H), 2.21 (dtd, $J = 14.5$, 4.3, 1.7 Hz, 1H), 2.80 (d, $J = 16.0$ Hz, 1H), 2.90 (d, $J = 16.0$ Hz, 1H), 3.08 (s, 3H), 3.44 (br. s, 1H), 3.57 (dd, $J = 10.7$, 7.3 Hz, 1H), 3.62 (m, 1H), 3.70 (dd, $J = 10.7$, 3.4 Hz, 1H), 3.79 (m, 1H), 5.55 (br. s, 1H), 5.73 (s, 1H); ^{13}C NMR (125 MHz, $CDCl_3$): $\delta = 18.5$, 19.7, 23.5, 24.9, 25.4, 25.8, 26.4, 26.7, 27.0, 27.2, 27.4, 27.9, 29.6, 30.8, 36.7, 57.6, 65.5, 100.3, 109.9, 130.5, 149.4, 171.6

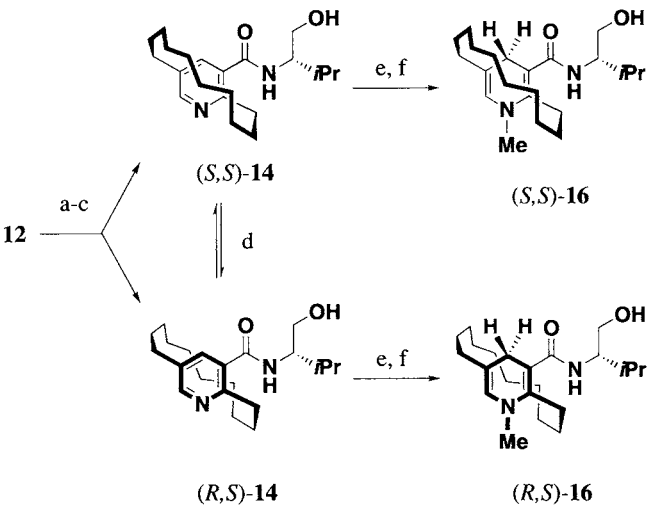

Scheme 3. Synthesis of (*S,S*)- and (*R,S*)-**16**. a) LiOH, $MeOH:H_2O$, RT, ca. 12 h; b) $SOCl_2$, DMF (cat.), Δ; c) (*S*)-valinol, Et_3N, $CHCl_3$, RT; d) toluene, Δ, 8 h; e) MeI, CH_3CN, Δ, 24 h; f) $Na_2S_2O_4$, CH_2Cl_2/aq. Na_2CO_3, 14 h.

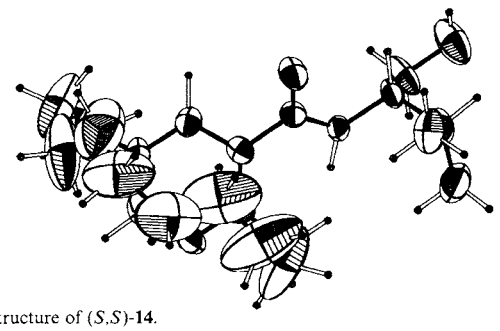

Figure 1. Crystal structure of (*S,S*)-**14**.

oligomethylene bridge is more dynamic than that of the pyridine and amide moieties. This result agrees with our design that the oligomethylene bridge would function as the bulky, shielding wall against substrate approach.

N-Alkylation of (*S,S*)- and (*R,S*)-**14** with methyl iodide afforded the corresponding *N*-methylpyridinium iodides (*S,S*)- and (*R,S*)-**15a** in quantitative yields. Regioselective 1,4-reduction of **15** by the biphasic reaction with aqueous sodium dithionite in dichloromethane resulted in the formation of (*S,S*)- and (*R,S*)-**16**.[17]

The bridged NADH models **16** were found to effect an excellent level of biomimetic reduction. The reaction of **16** with methyl benzoylformate was carried out in the presence of magnesium perchlorate in acetonitrile (Table 2). Stirring the reac-

Table 2. Reaction of methyl benzoylformate with **16** [a].

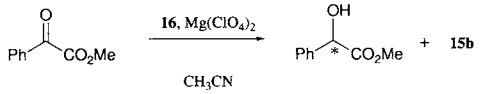

Entry	**16**	T [°C]	t	Methyl mandelate [b] config.	*ee* [%]	yield [%]	**15b** yield [%]
1	(*S,S*)-**16**	RT	5 d	*R*	99	64	66
2	(*S,S*)-**16**	50	24 h	*R*	99	70	81
3	(*S,S*)-**16**	75	6 h	*R*	98	63	65
4	(*R,S*)-**16**	RT	4 d	*S*	97	64	60
5	(*R,S*)-**16**	75	6 h	*S*	98	63	71

[a] Reaction conditions: 1.0 equiv **16**, 0.9 equiv methyl benzoylformate, 1.0 equiv $Mg(ClO_4)_2$, MeCN. [b] The enantiomeric excess was determined chromatographically with a Chiralcel OJ HPLC column (Daicel Chemical Technologies).

  0570-0833/97/3611-1209 $ 17.50+.50/0

tion mixture for 5 days at room temperature in the dark resulted in the desired hydrogen transfer from (*S,S*)-**16** to methyl benzoylformate, which occurred enantioselectively to afford (*R*)-methyl mandelate with 99% *ee* (64% yield) and the corresponding homochiral N-methylpyridinium perchlorate (*S,S*)-**15b** (66% yield; Table 2, entry 1). It is noteworthy that the rate of the reaction raised remarkably with increasing reaction temperature without significant decrease of enantioselectivity. The reactions were complete within 24 h at 50 °C and within 6 h at 75 °C to give (*R*)-methyl mandelate with 99% *ee* and 98% *ee*, respectively (entries 2 and 3).

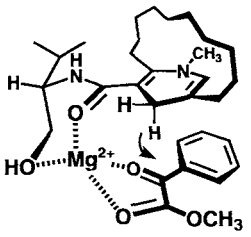

Scheme 4. Proposed transition state for the reduction of methyl benzoylformate with (*S,S*)-**16** in the presence of Mg^{2+}.

The estimated transition state for the asymmetric reduction with (*S,S*)-**16** is illustrated in Scheme 4. The ternary complex[18] in which magnesium perchlorate chelates to methyl benzoylformate beneath the bridged NADH model, since the top side of the model is blocked by the oligomethylene chain, rationalizes the enantioselectivity. The reactions of bridged NADH models proceeded stereospecifically. Reduction with (*R,S*)-**16** resulted in the formation of (*S*)-methyl mandelate with 97% *ee* at room temperature and 98% *ee* at 75 °C (64% and 63% yields, respectively; entries 4 and 5). Inouye et al.,[5a] Vekemans et al.,[2b] and Combret et al.[3b] studied the temperature effect of their NADH-model reactions and reported more or less decreased enantioselectivity with higher temperatures. The NADH model without a chelating group reported by Vekemans et al. reduced benzoylformate to mandelate in 95% optical yield at −25 °C, which dropped to 66% at 25 °C. Therefore, the chelating group derived from (*S*)-valinol in **16** apparently assists in stabilizing the ternary complex even at higher temperatures, as is reflected in the unique temperature independency of the enantioselectivity.

For reactions with NADH models with chiral amide moieties, the enantioselectivity of the asymmetric reduction is considerably dependent on the absolute configuration of the amide groups.[1a, 3, 4] Davies et al. reported NADH models with both a chiral amide group and a chiral ferocenyl group designed for selective shielding of their dihydropyridine rings.[4] However, there seems to be both matched and mismatched combinations between the two auxiliary groups, and, although the matched NADH models gave mandelate with 97–98% *ee*, the mismatched ones only gave 15–16% *ee*. On the other hand, in the case of **16** both diastereomers induced high enantioselectivity, which is strictly subject to the absolute structure of the solid parapyridinophane moieties. Therefore, the amide group derived from (*S*)-valinol does not behave as a "chiral auxiliary group" but simply as a "tight chelating group", and the absolute configuration has nothing to do with the selectivity. The salts **15b**, recovered by chromatography on silica gel, could be recycled to produce **16**, since the bridged NAD^+/NADH model system retains its plane chirality throughout the redox reaction. Consequently, the bridged NADH models designed from enzymatic environment successfully controlled both the direction and the orientation of substrate approach to induce high enantioselectivity in the biomimetic reactions.

Received: December 23, 1996 [Z 9920 IE]
German version: *Angew. Chem.* **1997**, *109*, 1263–1266

Keywords: asymmetric synthesis · macrocycles · NADH model compounds · pyridinophanes

[1] Reviews: a) G. Dupas, V. Levacher, J. Bourguignon, G. Quéguiner, *Heterocycles* **1994**, *39*, 405; b) V. A. Burgess, S. G. Davies, R. T. Skerlj, *Tetrahedron: Asymmetry* **1991**, *2*, 299.

[2] a) A. Ohno, M. Ikeuchi, T. Kimura, S. Oka, *J. Am. Chem. Soc.* **1979**, *101*, 7036; b) P. M. T. de Kok, L. A. M. Bastiaansen, P. M. van Lier, J. A. J. M. Vekemans, H. M. Buck, *J. Org. Chem.* **1989**, *54*, 1313; c) A. I. Meyers, T. Oppenlaender, *J. Am. Chem. Soc.* **1986**, *108*, 1989.

[3] a) Y. Combret, J. J. Torché, P. Binay, G. Dupas, J. Bourguignon, G. Quéguiner, *Chem. Lett.* **1991**, 125; Y. Combret, J. J. Torché, N. Plé, J. Duflos, G. Dupas, J. Bourguignon, G. Quéguiner, *Tetrahedron* **1991**, 47, 9369; b) Y. Combret, J. Duflos, G. Dupas, J. Bourguignon, G. Quéguiner, *Tetrahedron* **1993**, *49*, 5237; c) J. Bédat, V. Levacher, G. Dupas, G. Quéguiner, J. Bourguignon, *Chem. Lett.* **1995**, 327; *ibid.* **1996**, 359.

[4] V. A. Burgess, S. G. Davies, R. T. Skerlj, M. Whittaker, *Tetrahedron: Asymmetry* **1992**, *3*, 871; V. A. Burgess, S. G. Davies, R. T. Skerlj, *J. Chem. Soc. Chem. Commun.* **1990**, 1759; S. G. Davies, R. T. Skerlj, M. Whittaker, *Tetrahedron: Asymmetry* **1990**, *1*, 725.

[5] a) M. Seki, N. Baba, J. Oda, Y. Inouye, *J. Am. Chem. Soc.* **1981**, *103*, 4613; F. Hoshide, S. Ohi, N. Baba, J. Oda, Y. Inouye, *Agric. Biol. Chem.* **1982**, *46*, 2173; M. Seki, N. Baba, J. Oda, Y. Inouye, *J. Org. Chem.* **1983**, *48*, 1370; b) K. Skog, O. Wennerström, *Tetrahedron Lett.* **1992**, *33*, 1751.

[6] J. G. de Vries, R. M. Kellogg, *J. Am. Chem. Soc.* **1979**, *101*, 2759; P. Jouin, C. B. Troostwijk, R. M. Kellogg, *ibid.* **1981**, *103*, 2091; A. G. Talma, P. Jouin, J. G. de Vries, C. B. Troostwijk, G. H. Werumeus Buning, J. K. Waninge, J. Visscher, R. M. Kellogg, *ibid.* **1985**, *107*, 3981.

[7] S. Obika, T. Nishiyama, T. S., K. Miyashita, T. Imanishi, *Chem. Lett.* **1996**, 853; T. Imanishi, Y. Hamano, H. Yoshikawa, C. Iwata, *J. Chem. Soc. Chem. Commun.* **1988**, 473.

[8] NAD^+/NADH model compounds with pyridinophane skeletons: a) T. Oikawa, N. Kanomata, M. Tada, *J. Org. Chem.* **1993**, *58*, 2046; b) P. M. de Kok, H. M. Buck, *J. Chem. Soc. Chem. Commun.* **1985**, 1009; c) see ref. [6].

[9] Synthesis of [*n*](2,5)pyridinophanes: a) T. Kobayashi, M. Nitta, *Bull. Chem. Soc. Jpn.* **1985**, *58*, 3099; M. Nitta, T. Kobayashi, *Tetrahedron Lett.* **1984**, *25*, 959; b) H. Gerlach, E. Huber, *Helv. Chim. Acta* **1968**, *51*, 2027; application of [*n*](2,5)pyridinophanes as vitamin B6 models: c) J. T. Koh, R. Breslow, *J. Am. Chem. Soc.* **1994**, *116*, 11234; d) T. Tachibana, M. Ando, H. Kuzuhara, *Bull. Chem. Soc. Jpn.* **1983**, *56*, 3652; H. Kuzuhara, M. Iwata, S. Emoto, *J. Am. Chem. Soc.* **1977**, *99*, 4173.

[10] Aldehyde **1** was prepared from cyclododecanone by Vilsmeier–Haack formylation in 55% yield: ^{1}H NMR (500 MHz, $CDCl_3$): δ = 1.25 (m, 2H), 1.36–1.47 (m, 10H), 1.51 (m, 2H), 1.84 (m, 2H), 2.37 (t, J = 7.6 Hz, 2H), 2.65 (t, J = 7.5 Hz, 2H), 10.24 (s, 1H); ^{13}C NMR (125 MHz, $CDCl_3$): δ = 22.2, 22.8, 23.8, 24.5, 24.87, 24.90, 25.1, 25.3, 26.4, 34.3, 135.9, 154.7, 192.7.

[11] **2**: IR (neat): $\tilde{\nu}$ = 2932, 1778, 1702 cm^{-1}; ^{1}H NMR (500 MHz, $CDCl_3$): δ = 1.11–1.56 (m, 14H), 1.72 (m, 1H), 1.80 (ddd, J = 13.7, 9.0, 6.0 Hz, 1H), 2.00 (m, 1H), 2.12 (ddd, J = 13.7, 7.7, 6.0 Hz, 1H), 2.88 (ddd, J = 16.7, 7.7, 4.7 Hz, 1H), 3.03 (ddd, J = 16.7, 9.2, 4.5 Hz, 1H), 8.77 (s, 1H); ^{13}C NMR (125 MHz, $CDCl_3$): δ = 21.9, 22.8, 23.2, 24.6, 24.9, 25.4, 25.5, 25.8, 26.6, 26.7, 48.4, 167.5, 201.1.

[12] Carboxaldehyde **3** was isolated by thin-layer chromatography (TLC) on aluminum oxide with chloroform/hexane (2/1) as eluent: IR (neat): $\tilde{\nu}$ = 2103, 1661, 1599 cm^{-1}; ^{1}H NMR (500 MHz, $CDCl_3$): δ = 1.12–1.34 (m, 10H), 1.35–1.52 (m, 3H), 1.58–1.83 (m, 3H), 2.27 (ddd, J = 13.3, 8.3, 3.0 Hz, 1H), 2.39–2.45 (m, 2H), 3.35 (ddd, J = 14.5, 8.6, 4.1 Hz, 1H), 9.94 (s, 1H); ^{13}C NMR (125 MHz, $CDCl_3$): δ = 23.3, 23.4, 23.5, 23.6, 23.9, 25.4, 26.3, 26.4, 26.8, 27.0, 129.6, 156.3, 189.4.

[13] Formation of *cis*-2-azidocyclododecene-1-carboxaldehyde by the reaction at 0 °C was confirmed by ^{1}H NMR spectroscopy. Heating the products to room temperature caused rapid transformation of the *cis*-azide into azirine **2**.

[14] Staudinger reaction of *trans*-azide **3** with triphenylphosphane afforded iminophosphorane **4** at room temperature in 48% yield. *trans*-**4**: ^{1}H NMR (500 MHz, $CDCl_3$, −50 °C): δ = 0.36 (m, 1H), 0.84–1.53 (m, 14H), 1.74 (t, J = 11.6 Hz, 1H), 1.83 (t, J = 11.5 Hz, 1H), 2.59 (t, J = 11.5 Hz, 1H), 2.84 (m, 1H), 3.21 (m, 1H), 7.55 (td, J(H,H) = 8.1, J(H,P) = 2.7 Hz, 6H), 7.63 (t, J = 8.1 Hz, 3H), 7.82 (dd, J(H,H) = 8.1, J(H,P) = 12.4 Hz, 6H), 9.80 (s, 1H); ^{13}C NMR (125 MHz, $CDCl_3$, −50 °C): δ = 21.8, 22.0, 22.5, 22.6, 23.2, 24.7, 26.2, 26.4, 29.2, 34.7 (d, J(C,P) = 8.6 Hz), 124.4 (d, J(C,P) = 17.2 Hz), 128.7 (d, J(C,P) = 17.2 Hz, 6C), 129.9 (d, J(C,P) = 101.0 Hz, 3C), 132.2, 132.5 (d, J(C,P) = 9.7 Hz, 6C), 187.8; *cis*-**4**: ^{1}H NMR (500 MHz, $CDCl_3$, −50 °C): δ = 2.30 (m, 2H), 2.55 (m, 2H), 7.52 (dt, J(H,H) = 7.7, J(H,P) = 3.0 Hz, 6H), 7.61 (m, 3H), 7.78 (m, 6H), 10.86 (s, 1H), other signals (16H) are hidden by those of *trans*-**4**.

[15] The configuration of the C=C bond was assigned by comparison with the ^{1}H NMR spectrum of the known formyl-substituted (vinylimino)phosphorane with a cyclohexene ring. The aldehyde group of the compound with exclusive *cis*-configuration is reported to appear at δ = 10.66 in [D_6]DMSO. We prepared this compound and confirmed that the chemical shift in $CDCl_3$ is δ = 10.72: B. Tabyaoui, T. Aubert, M. Farnier, R. Guilard, *Synth. Commun.* **1988**, *18*, 1475.

  0570-0833/97/3611-1210 $ 17.50+.50/0

[16] Crystal structure data of (*S,S*)-**14**: $C_{21}H_{34}N_2O_2$, M_r = 346.50, colorless plate, R = 0.074, R_w = 0.069. Crystallographic data (excluding structure factors) for the structures reported in this paper have been deposited with the Cambridge Crystallographic Data Centre as supplementary publication no. CCDC-100106. Copies of the data can be obtained free of charge on application to The Director, CCDC, 12 Union Road, Cambridge CB21EZ, UK (fax: int. code +(1223)336-033; e-mail: deposit(*a*) chemcrys.cam.ac.uk).

[17] The dihydropyridines **16** were used in the next step without further purification. These compounds are apparently sensitive to oxygen.

[18] Y. Toyooka, T. Matsuzawa, T. Eguchi, K. Kakinuma, *Tetrahedron* **1995**, *51*, 6459.

Enzymatic Resolution of Alcohols Coupled with Ruthenium-Catalyzed Racemization of the Substrate Alcohol**

Anna L. E. Larsson, B. Anders Persson, and Jan-E. Bäckvall*

Dedicated to Professor Henri B. Kagan

The resolution of racemic compounds by enzyme-catalyzed reactions has become a powerful tool in organic synthesis.[1, 2] In particular, processes for hydrolysis of esters and acylation of alcohols have been successfully employed. One limitation with classical enzymatic resolution is that the reactions are associated with a maximum yield of 50% based on the racemate. In order to overcome this limitation the substrate could be continuously racemized during the resolution process; this would lead to efficient use of all of the starting material. This approach has attracted some interest recently, and a few applications have been reported.[2–6]

During our studies on ruthenium-catalyzed hydrogen transfer reactions we observed that alcohols undergo fast isomerization at the α-carbon leading to racemization or epimerization.[7–9] Attempts to use chiral ligands in order to obtain ruthenium-catalyzed asymmetric transfer hydrogenations were hampered by the racemization of the product,[10] and this has also been observed by others using the same catalytic system.[11] In connection with previous enzyme studies in our group[12] we decided to investigate enzymatic resolution of racemic alcohol mixtures coupled with the above-mentioned racemization. In this communication we report on the successful enzymatic resolution of alcohols under substrate-racemizing conditions (second-order asymmetric transformation[13]) (Scheme 1).

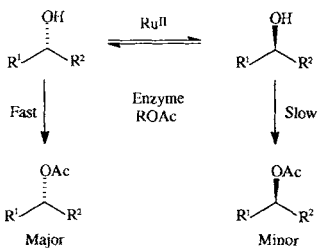

Scheme 1. Enzymatic resolution under substrate-racemizing conditions.

[*] Prof. J.-E. Bäckvall, A. L. E. Larsson, B. A. Persson
Department of Organic Chemistry
Uppsala University
Box 531, S-75121 Uppsala (Sweden)
Fax: Int. code +(18)-508-542
e-mail: jeb(*a*) kemi.uu.se

[**] We would like to thank Dr. Ratan. L. Chowdhury who performed the initial studies on the racemization of alcohols. *Candida antarctica* component B Lipase (Novozym 435) was a gift from Novo Nordisk A/S, Denmark. Financial support by the Swedish National Science Research Council is gratefully acknowledged.

Catalytic amounts of $[(PPh_3)_3RuCl_2]$ (**1**) epimerized *cis*-2-methylcyclohexanol and racemized enantiomerically pure α-methylbenzyl alcohol ((+)-(*R*)-**3**). For an efficient isomerization it was necessary to use a ketone as a cocatalyst to promote the ruthenium-catalyzed hydrogen transfer reactions.[9a] Consequently, the corresponding ketones, 2-methylcyclohexanone and acetophenone, were used. The epimerization of *cis*-2-methylcyclohexanol proceeded with a moderate rate,[14] whereas the racemization of (+)-(*R*)-**3** took only 4 h with 2 mol% of the catalyst in the presence of base (Scheme 2). The latter reaction was quite sensitive, and in some of the reactions the catalyst was deactivated and racemization stopped.

Because of the problems with the reproducibility of catalyst **1** we turned our attention to ruthenium catalyst **2**.[15] This catalyst

$[(PPh_3)_3RuCl_2]$

1

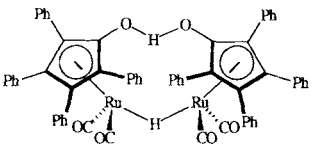

2

has been found to be less sensitive and can be used over longer reaction periods without being deactivated.[9c, d] Reaction of (+)-(*R*)-**3** in the presence of 2 mol% of catalyst **2** and 1 equivalent of acetophenone in *t*BuOH at 70 °C led to a complete racemization in 45 h (Scheme 2).

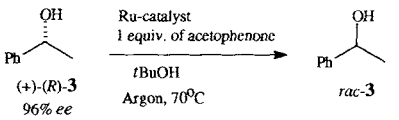

Scheme 2. Ruthenium-catalyzed racemization of (+)-(*R*)-**3**. Reaction conditions: 2 mol% of **1**, 10 mol% of NaOH, 4 h or 2 mol% of **2**, 45h.

The ruthenium-catalyzed racemization of (+)-(*R*)-**3** was combined with an enzyme-catalyzed transesterification with *Candida antarctica* component B lipase (Novozym 435 = N-435).[16] The use of catalyst **1** in combination with the enzyme and the acyl donor gave poor results, and the rapid racemization with this catalyst could not be reproduced in the presence of the enzyme. Combination of catalyst **2** and the enzyme worked better (Eq. (a) and Table 1). We first tried vinyl acetate as the

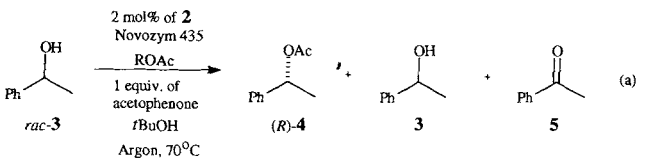

acyl donor. Although a complete conversion of the alcohol took place, only about 50% of the acetate was obtained, because the acetaldehyde formed when using this acyl donor reacts as a hydrogen acceptor and oxidizes the substrate alcohol to ketone.[17]

The use of isopropenyl acetate, from which acetone is formed in the acylation step, showed the same phenomenon but to a lesser extent than for vinyl acetate. In this case 72% of the substrate was converted into (*R*)-α-methylbenzyl acetate ((*R*)-**4**), and the remaining 28% was oxidized (Table 1, entry 2). The